

# Total harmonic distortion optimization of the line voltage in single source cascaded multilevel converter

LUIS DAVID PABON, JORGE LUIS DIAZ RODRIGUEZ, ALDO PARDO GARCIA.

Department of Electrical Engineering and Mechatronics

University of Pamplona.

Ciudadela Universitaria, Km. 1, via Bucaramanga, Pamplona.

COLOMBIA

davidpabon@unipamplona.edu.co, jdiazcu@unipamplona.edu.co, apardo13@unipamplona.edu.co

*Abstract:* - This paper describes the harmonic content optimization process of the line voltage in a three-phase H-bridge cascaded multilevel converter with single source topology and 9 levels per phase voltage and 15 levels per line voltage. For optimization reason it was developed a mathematical expression to calculate the line voltage THD in terms of switching angles at the first quarter of the phase voltage modulation waveform. Then problem becomes purely numerical and it's solved using a genetic algorithm, which allows finding a modulation with a THD value close to zero. In order to verify the simulation results, a multilevel power converter with the mentioned topology was developed and its performance tested, with different types of loads.

*Key-Words:* - Multilevel power inverter, multilevel PWM modulation, H-bridges cascaded single source, THD, genetic algorithm, optimization.

## 1. Introduction

Nowadays there is a profound interest of generating high standard electricity through alternative energy sources, this is due to environmental disasters caused by many factors, one of them is the conventional sources of energy, in this context solar energy has been widely accepted because of its many advantages as a source of renewable energy and has presented a continuous growth in recent years [1], settling large number of photovoltaic (PV) systems around the world [2].

The production of electricity from solar panels is given in direct component, using power inverters is a complete solution to convert AC voltage output [3] for the use of energy or connecting to the power network [2]. However, conventional converters used in this application have certain problems in terms of power quality, due to harmonic distortion [4], [5].

Since in photovoltaic (PV) systems into alternating the power quality depends on the power inverter [6], today there have been numerous investigations aimed on optimizing the harmonic content of these [7], [8], presenting multilevel converters as a solution to the problem, because these inverters have many advantages compared with conventional two levels: waveforms of high quality energy, low loss switching capacity of high voltage, low electromagnetic interference, etc. [9]-[11]. In this way exclusive area harmonic content optimization of PV systems through multilevel converters works are presented [12]-[14].

This research through using genetic algorithms aims to optimize the harmonic content of the three phase photovoltaic systems, minimizing THD line directly through a cascaded asymmetric H-bridge single source multilevel power converter [15] nine levels phase adopt the modulation found by the optimization algorithm.

## 2. A review

The multilevel power converter appears in the year 1975 with Baker and Lawrence patent [16], performing the first implementation in 1981 [17], from these works, numerous investigations have come to get a variety of converters [11] some of which are considered as classics [3]: clamped diodes, flying capacitor and cascaded H-bridges. In the same way recently topologies that are considered innovative and seek to reduce the number of components, increase efficiency or improve power quality have appeared [18]-[20].

Inside the classic topologies, the cascade H-bridges is considered advantageous in terms of quality of the waveform and number of components [3], within this a convenient sub-topology appears in photovoltaic systems using an accumulator block, because it uses a single voltage source directly, accompanied by a transformer at the output of the H-bridge, this topology is named as a cascaded H-bridge multilevel converter with single source [21].

This configuration is very suitable for low cost renewable energy applications, because it feeds the entire system from a single source [9]. However, using a transformer to the output, creates problems in terms of the perturbation of the waveform and makes the system even more complex [9], [22]. Problems have been studied and have been solved in works like [6] and [23].

In the field of harmonic content optimization of modulations in multilevel power converters there have been several proposed techniques depending on the topology used, the specific objective and the shape of the search for an optimum [24], [25], however there are very promising strategies in the line of evolutionary algorithms and particle swarm (PSO) and genetic algorithms (GA) [8], some of these studies conclude that outperforms genetic algorithms [8] and [26].

Similarly these optimizations mostly made in the phase voltages of the converters [15], [28], [29] and very few are made directly in the line voltages [30] reaching results not so near from zero. For these reasons in this paper a multilevel converter H-bridges single source cascade that optimizes THD of line voltages directly, using genetic algorithms, as proposed to improve power quality three-phase PV systems is presented.

### 3. Single Source multilevel inverter of nine steps per phase

The topology of multilevel power inverter selected for this work is the 2 stages H-bridge asymmetrical cascaded with single source and 1:3 ratio. Which generates 9 levels of output voltage of each phase, this topology is shown in Figure 1.

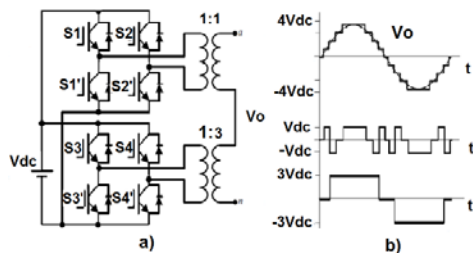


Fig. 1. Asymmetry two stages cascaded power inverter in single source with 9 levels at the output, asymmetry 1: 3 Topology. b) Vout.

This converter allows a minimum of stages of H-bridges (2 steps) to achieve the possible maximum number of output voltage steps (9 steps). The Figure 2 shows the three-phase topology, which is the triplication of the single phase presented in Figure 1. As shown, the three phases share the DC bus.

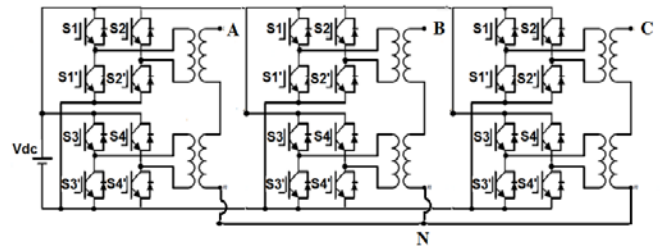


Fig. 2. Converter topology.

The waveform generated by the phase converter shown in Figure 3. This voltage waveform is achieved if phase-multilevel PWM modulation is generated. It is expected that the line voltage converter has more steps and more pulses due to the subtraction between phase voltages, this will be shown in later sections.

### 4. Mathematical modeling

In this study obtained an expression that quantifies the total harmonic distortion of line voltages in terms of switching angles of each step of the phase voltage, both: the *on* and *off* angles.

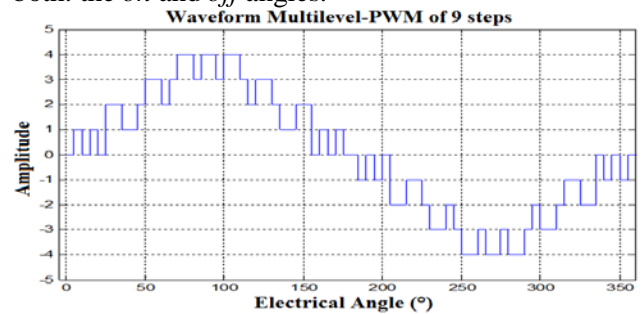


Fig. 3. 9 steps PWM modulation waveform.

In order to determine this equation it was modeled using Fourier phase voltages A and B series of an ABC phase system of 9 steps PWM modulations. Since the line voltage is the subtraction of the phase voltages (on a connection and for the converter), the Fourier series of the line voltage is obtained by the respective difference. Getting the Fourier series of line voltage THD is calculated in terms of the first 50 harmonics following the IEEE-519 standard [31].

#### Phase A

As the shape of the modulation shown in a quarter (1/4) keeping the symmetry of the waveform, it is only necessary to define the switching angles in the first quarter wave (Fig. 4), the remaining parts of the modulation are constructed using trigonometric relationships. Thus a vector  $L = [a \ b \ c \ d]$  representing the total number of switch on and switch off angles at each step is established. The Fourier series for periodic waveforms states:

$$v(t) = \frac{a_0}{2} + \sum_{n=1}^{\alpha} (a_n \cos n\omega_0 t + b_n \sin n\omega_0 t) \quad (1)$$

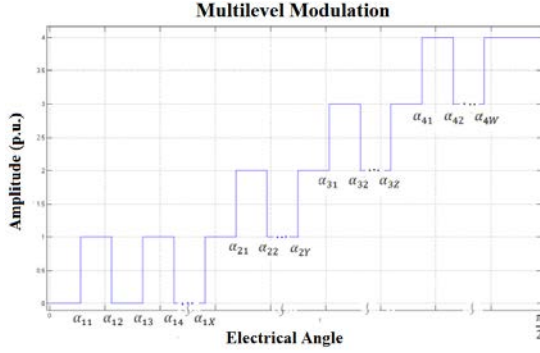


Fig. 4. A quarter of a modulation waveform in terms of switch *on* and switch *off* of each step angles.

Where  $n$  is the harmonic number,  $\omega_o$  the fundamental frequency wave, time  $t$ ,  $a_0/2$  is the DC component, which is calculated by the expression:

$$a_0 = \frac{1}{2\pi} \int_0^{2\pi} v(\omega t) d(\omega t) \quad (2)$$

$a_n$  coefficient of the Fourier series is calculated

$$\text{with (3): } a_n = \frac{1}{\pi} \int_0^{2\pi} v(\omega t) \cos n(\omega_0 t) d(\omega t) \quad (3)$$

$b_n$  coefficient of the Fourier series, calculated by:

$$b_n = \frac{1}{\pi} \int_0^{2\pi} v(\omega t) \sin n(\omega_0 t) d(\omega t) \quad (4)$$

The waveform (Fig. 4) presents uneven symmetry and the positive part is equal to the negative applying thereby, symmetries as the theory of Fourier series.

$$a_o = 0 \text{ and } a_n = 0 \quad (5)$$

Only the coefficient related within the sinus will remain, therefore the waveform in terms of the Fourier series, will be expressed as follows:

$$v(t) = \sum_{n=1}^{\alpha} b_n \sin n\omega_0 t \quad (6)$$

$b_n$  in terms of  $L$  vector for waveform:

$$b_n = \frac{4v_{cd}}{n\pi} \left[ \sum_{i=1}^4 \sum_{j=1}^{L_i} (-1)^{j-1} \cos n\alpha_{ij} \right] \text{ for odd } n; \quad (7)$$

and  $b_n = 0$  for even  $n$ .

Where  $i$  is the number of the step (hence the sum is from 1 to 4),  $L_i$  the vector's  $i$  component  $L$  and  $\alpha_{ij}$  the  $j$  angle of the  $i$  step, this can be switch on or switch off. For a ladder vector components  $L$  must be odd. If the peak magnitude of harmonic  $n$ , in the Fourier series is defined as:

$$h_n = \sqrt{a_n^2 + b_n^2} \quad (8)$$

Substituting (5) and (7) (8) the peak magnitude of each harmonic  $n$ , where only odd harmonics will exist because  $b_n=0$ , if  $n$  is even therefore obtained as:

$$h_n = \frac{4v_{cd}}{n\pi} \left[ \sum_{i=1}^4 \sum_{j=1}^{L_i} (-1)^{j-1} \cos n\alpha_{ij} \right] \text{ for } n = 1, 3, \dots, \quad (9)$$

The expression in the form of Fourier series phasors of a waveform in terms of the fundamental and harmonic component:

$$v(t) = a_0 + \sum_{n=1}^{\alpha} h_n \sin(n\omega t + \varphi_n) \quad (10)$$

Where  $a_0$  is the direct component,  $h_n$  the amplitude for each harmonic calculated in (9) and  $\varphi_n$  the phase of each harmonic calculated in (11):

$$\varphi_n = \tan^{-1} \frac{a_n}{b_n} \quad (11)$$

For this case  $\varphi_n$  and null  $a_0$  and therefore the associated terms for the Fourier series for phase A, in the form of equation (10), are:

$$h_n = \begin{cases} 0 & \text{for even } n \\ \frac{4v_{dc}}{\pi n} \sum_{i=1}^4 \sum_{j=1}^{L_i} (-1)^{j-1} \cos n\alpha_{ij} & \text{for odd } n \end{cases} \quad (12)$$

$$\varphi_n = 0 \quad (13)$$

### Phase B

Determining the Fourier series of phase B of the ABC system, the A waveform from Fig. 3 was phase shift of 120 degrees, this corresponds to each angle presented in Fig. 4 should be shifted  $2\pi/3$  rad, and due to this displacement the odd symmetry is not applicable to this waveform, thus following the same process of A phase it is possible to calculate the Fourier series of the phase B but in this case should be calculated on the  $a_n$  and  $b_n$  full cycle.

The shifted phase wave form still has symmetry about the x-axis component thus direct voltage remains null Phase B:

$$a_o = 0 \quad (14)$$

The terms associated for the Fourier series for phase B, in the form of equation (10), are those shown in (15) and (16):

$$C_n = \begin{cases} 0 & \text{for even } n \\ \frac{4v_{dc}}{\pi n} \left( \sum_{i=1}^4 \sum_{j=1}^{L_i} (-1)^{j-1} \cos n\alpha_{ij} \right) & \text{for odd } n \text{ (multiple of 3)} \\ \frac{4v_{dc}}{\pi n} \left( \sum_{i=1}^4 \sum_{j=1}^{L_i} (-1)^{j-1} \cos n\alpha_{ij} \right) & \text{for odd } n \text{ (non multiple of 3)} \end{cases} \quad (15)$$

$k$  represents the number of odd harmonic not multiple of 3, for example  $k=1, n=5, k=2$  to  $n=7, k=3$  to  $n=11$ , so on.

### Line Voltage

For calculating the Fourier series in the line voltages set out from the Fourier series of the voltages phase difference:

$$v_{AB}(t) = v_A(t) - v_B(t) \quad (16)$$

By making the respective differences of the Fourier series of Phases A and B, in the forms of equation (10) with the amplitudes and offsets given by (12), (13), (15) and (16) the Fourier series for  $v_{AB}$  line voltage is obtained, but in the article only the harmonic amplitude is presented, since the objective is to minimize THD and for this mismatch harmonics are required, therefore the harmonic amplitudes of the line voltages shall be expressed by equation (17):

$$h_n = \begin{cases} 0 & \text{for even } n \\ 0 & \text{for odd } n \text{ (multiple of 3)} \\ \frac{4\sqrt{3}v_{\phi}}{\pi n} \left( \sum_{i=1}^4 \sum_{j=1}^{L_i} (-1)^{j-1} \cos n\alpha_{ij} \right) & \text{for odd } n \text{ (non multiple of 3)} \end{cases} \quad (17)$$

**Line voltage THD**

The IEEE 519 standard in 1992 on page 63 [31] defines the total harmonic distortion as equation 10:

$$THD = \frac{\sqrt{\sum_{n=2}^{50} h_n^2}}{h_1} \cdot 100 \quad (18)$$

Where  $h_1$  is the fundamental harmonic component and  $h_n$  the peak of the harmonic  $n$ . Replacing (17) in (18):

$$THD = \frac{\sqrt{\sum_{n=2}^{50} \left( \frac{1}{n} \left[ \sum_{i=1}^4 \sum_{j=1}^{L_i} (-1)^{j-1} \cos n\alpha_{ij} \right] \right)^2}}{\left[ \sum_{i=1}^4 \sum_{j=1}^{L_i} (-1)^{j-1} \cos \alpha_{ij} \right]} * 100 \quad (19)$$

Where  $n$  takes not odd values non multiple of 3, i.e. 5, 7, 11, 13, 17, etc. and  $L_i$  are the components of the vector  $L = [a b c d]$ . Thus (19) defines the fitness function to be minimized by the optimization algorithm.

**5. Optimization Algorithm**

With the help of Matlab® and GA command (Genetic Algorithm) algorithms for the mathematical model of the fitness function (Equation 19) and its respective optimization using genetic algorithms were programmed. The size of the population for the algorithm is taken from 20 individuals, each individual ( $X$ ) consists of the total of switching angles in the first quarter voltage waveform:

$$X = [\alpha_{1x} \alpha_{12} \dots \alpha_{1x} \alpha_{21} \alpha_{22} \dots \alpha_{2y} \alpha_{31} \dots \alpha_{3z} \alpha_{11} \dots \alpha_{1w}] \quad (20)$$

The  $L$  vector indicates the values obtained in the evaluation of the fitness function (angles) corresponding to each step. The algorithm flowchart is shown in Fig. 5.

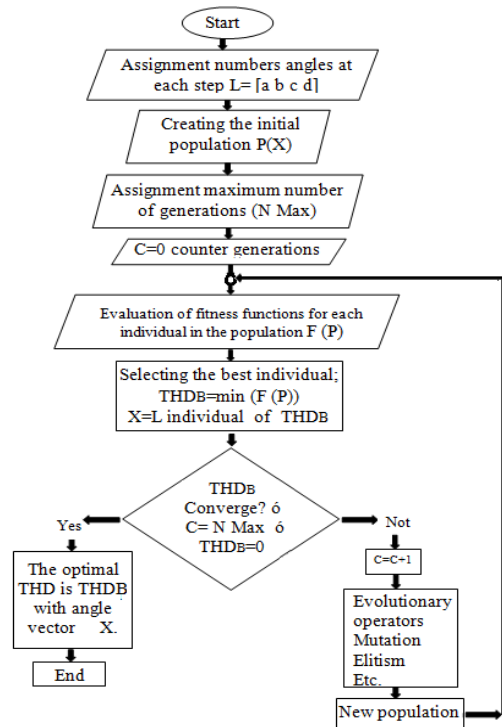


Fig. 5. Optimization algorithm flowchart.

**6. Results**

$L = [3 3 5 9]$  is the vector which defines the number of switching angles in each step indicating that the first and second step have a pulse and a half, in the third step two pulses and a half, in the last step 4 pulses and a half in the first quarter wave voltage phase. The switching phase angles are summarized in Table I

TABLE I: ANGLES OF THE BEST INDIVIDUAL.

a=3	b=3	c=5	d=9	
5.70241538	18.229993	34.4310184	53.386964	73.2043847
9.94093425	24.218687	34.7242607	55.288426	73.2387503
12.51467958	26.1824422	36.5706369	60.479581	78.4542332
		45.0850569	64.6966	81.6462089
		47.1467285	67.878653	

The THDv of line voltages of a balanced three-phase system which uses a nine steps phase modulation with shooting previous fire angles theoretically will be of 0.000132%. THDv introduced a phase of 10.8631%. In Figure 6 the  $v_A$  waveform voltage phase is shown, and in Figure 6.b its harmonic spectrum.

Figure 6, b shows that the harmonics appearing in the phase modulation are tripling, because of this the THD phase is high (10.8631%), these harmonics are deleted in the line voltage at withdrawing the two positive sequence phases. The waveforms of three-phase line modulations obtained by subtracting the

phases of the positive sequence waveforms is shown in Figure 6, shown in Figure 7.a and its spectrum is shown in Figure 7.b.

As shown in Figure 7.a, there in the line voltage appear additional steps due to the subtraction done between the phases, phase modulation has nine steps, while the line has 15 steps, similarly more pulses occur, and this makes the waveform get closer to the sinusoidal and therefore the harmonic content decreases reaching a value of 0.000132%.

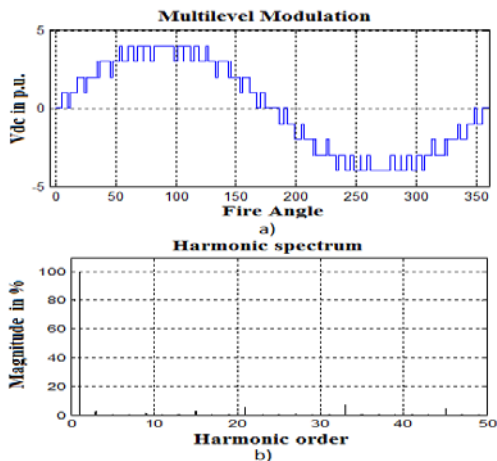


Fig. 6. Phase modulation. a) Waveform. b) Harmonic spectrum.

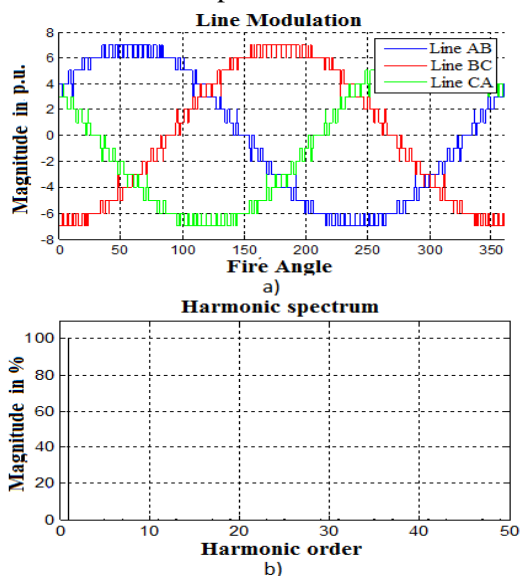


Fig. 7. Line Modulation. a) Waveform. b) Harmonic spectrum.

## 7. Implementation

In order to validate, a three-phase inverter prototype was implemented according to the topology selected in section III, based on the use of MOSFETs as switching devices. The power converter is rated 2100 VA, the input voltage  $48 V_{dc}$ , aimed to be applicable to low cost photovoltaic systems in which

only an accumulator block for this voltage is taken, the 60 Hz nominal frequency, and a nominal output voltage of 127 Vrms and 220 Vrms phase line. The control of converter is performed only with twelve signals, necessary to control the upper MOSFETs of the bridges, the lower is controlled by the denial of the 12 signs of major control and allocation of downtime was made along with the denial through hardware.

The control device in the experimental stage was based on the use of FPGAXUPV5-LX110T. The design of transformers, critical devices in achieving the waveform, raised according to the methodology proposed in [23]. Figure 8.a shows the converter stages.

## 8. Experimental setup

Figure 8.b shows assembly for the experimental tests carried out, here is possible to observe the basic components of the inverter: H-bridges, transformers, driver stage and FPGA. The analyzer power quality Fluke 434 and the 125 Fluke oscilloscope: the accumulator block, represented by laboratory sources from which the drive and measuring equipment are fed is also observed.

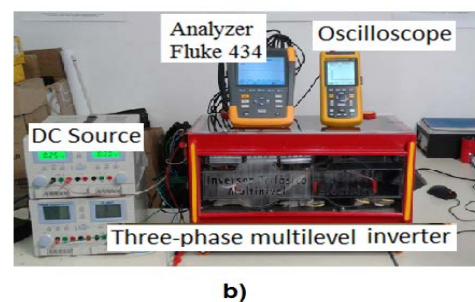
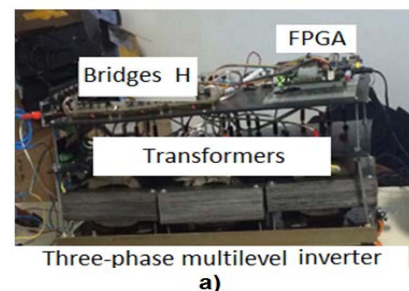


Fig. 8.a) Converter without housing b) Experimental tests mounting with a FPGA.

With the above assembly waveforms, RMS values, THD, phasor diagrams of the phase voltages and line, as the output currents of the inverter, for testing in vacuum, resistive load (resistive load of 250W), inductive load (1 Hp induction motor) and capacitive load (250W and 150 VAR) in order to verify the harmonic content of the implemented modulations.

**No-load test**

In order to verify the proper operation of the converter to replicate the waveforms calculated, the test was performed without inverter load.

Figure 9.a shows the line voltage waveform at the converter output without load. The spectrum obtained by the analyzer is shown in figure 9.b. This figure was expanded showing the ordinate axis with 20% (fig. 9.c) supporting the evidence that there is no harmonic), also, the spectrum of the phase voltage is presented to show the presence of harmonics in the phase and demonstrate effectively that optimization is done directly on the line voltage. In Figure 9.a. all pulses are not seen due to the display resolution of the analyzer.

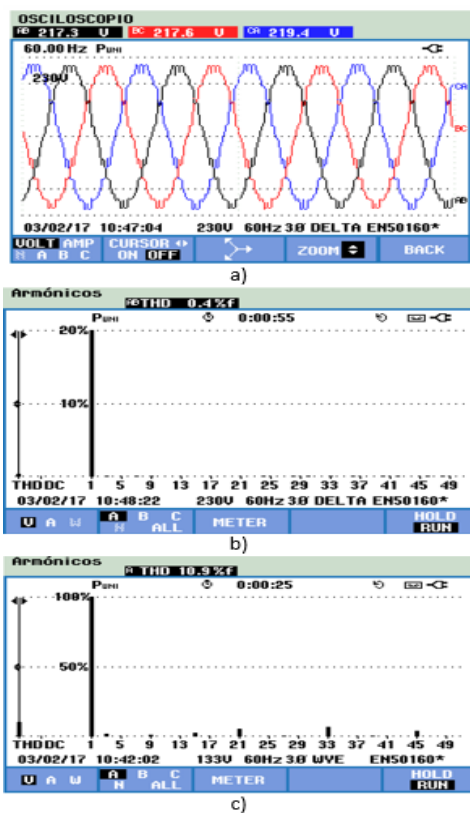


Fig. 9.a) Line voltage waveform. b) Spectrum. c) Phase voltage spectrum.

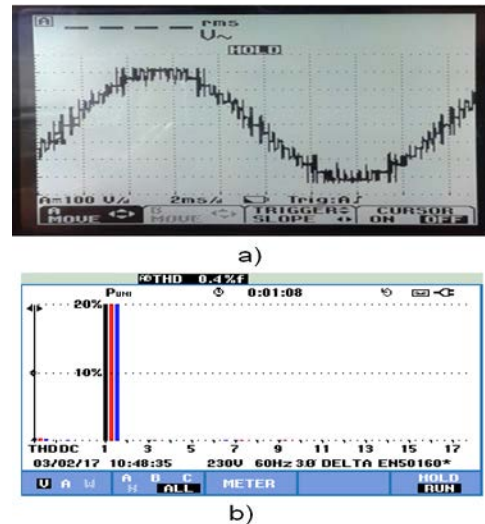


Fig. 10.a) Line voltage waveform b) Line voltages spectrum.

The figure 10.a shows the shape of the line voltage waveform captured by the oscilloscope in which the presence of all pulses is observed. In figure 10.b the spectrum is shown to the three-phase line voltages.

**Unity power factor test**

Figure 11.a shows the waveform of the three line voltages, it is observed that the system is a three-phase, balanced and positive sequence. In Figure 11.b The spectrum of line voltage is shown, where there is no significant contribution in the first fifty harmonics, this leads to the THD measured by the network analyzer is 0.3%, that fully complies with the IEEE 519 standard.

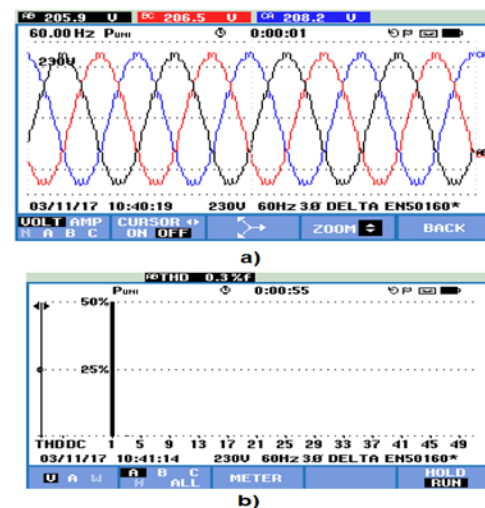


Fig.11.a) Line voltage waveform. b) Line voltages spectrum with resistive load.

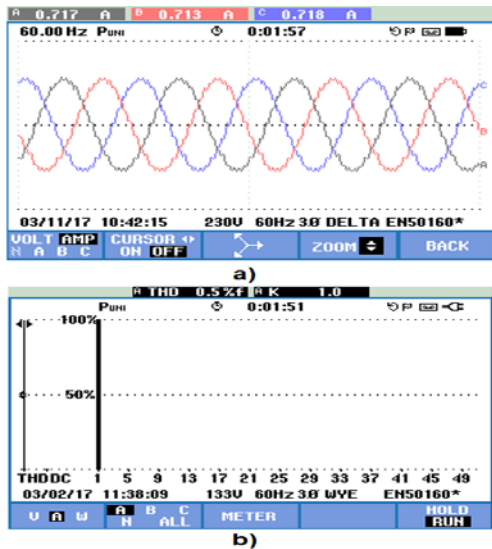


Fig. 12.a) Line current waveform b) Line current spectrum with resistive load.

Regarding the electrical current, in Figure 12.a it can be observed the current waveforms at three-phase lines. In Figure 12.b The harmonic spectrum is shown by the performed optimization at the line voltage. For this type of load; the THDi is 0.5%, which verifies the harmonic content optimization of the first 50 components.

Figure 13 shows the phasor diagram of voltages and currents measured in the test, you can see that the system has small unbalances in the voltage and the current. The voltage unbalance in line voltages has a value of 0.64% and the current unbalance 0.41%. These unbalance percentages comply with the 2%, range allowed by EN-50160.

Voltage regulation is estimated at 5.15% compliant with the IEEE-1159 standard, which states that the normal voltage operating range must be within 10% fluctuation respect to the rated voltage.

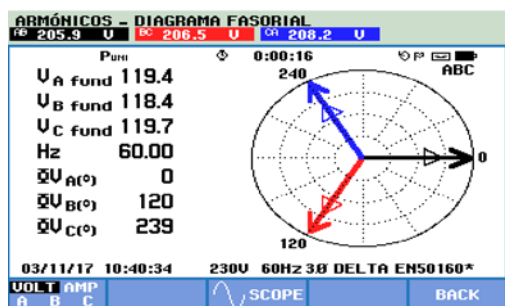


Fig.13. Phasor diagram for resistive load.

**Lag power factor test**

In Figure 14.a the waveform of the three line voltages is shown, it can be observed that the system in the presence of inductive loads remains balanced.

In Figure 14.b the spectrum of line voltage is shown. It can be observed that there is no significant contribution in the range of the first fifty harmonics. This leads to the THD measured by the network analyzer is 0.6%, twice as presented to resistive loads. However this THD is appropriate and fully complies with the IEEE-519 standard.

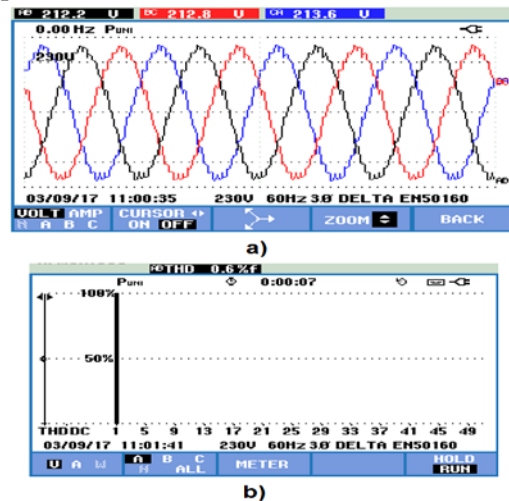


Fig.14.a) Line voltage waveform b) Line voltages spectrum with inductive load.

The figure 15.a shows the current, it can be observed that the ripple disappears. However, as shown in Figure 15.b the harmonic content increases due to the presence of low order components. Despite the THDi increases, it is only 2.3%, which confirms the optimization of the harmonic content in the first 50 components.

The phasor diagram of the measured voltages and currents in the test is shown in Figure 16. Although at first glance the system seems balanced, there are small differences in the voltages and currents. The unbalance of the line voltages has a value of 0.34%, much lower than in the resistive test and the current is 2.68%. Quite high due to voltage unbalance motor. Voltage regulation has a value of 1.97%, being below the value obtained in the resistive test and fully complies with the IEEE-1159 standard.

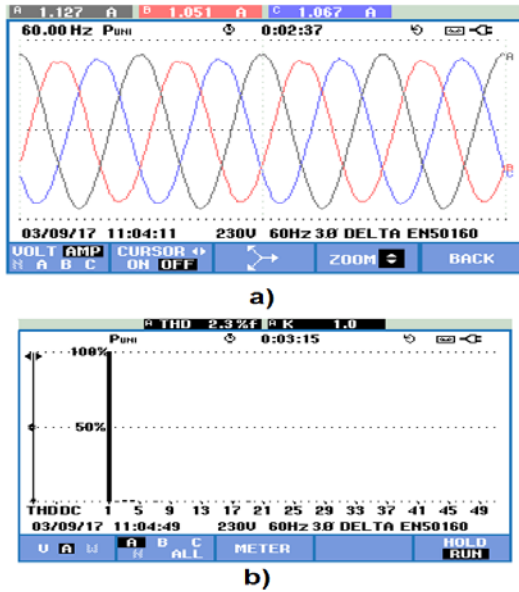


Fig. 15.a) Line current waveform b) Line current spectrum with inductive load.

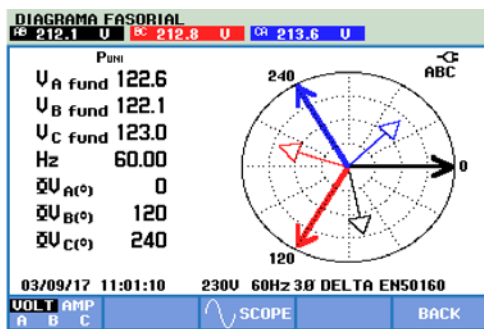


Fig.16. Phasor diagram for inductive load.

**Lead power factor test**

An RC load was used as last test to complete the optimization verification of the power converter. In Fig 17.a. the waveforms of the line voltages is shown. In Figure 17.b. the harmonic spectrum is shown. The THDv is 0.3%, clearly shows that the harmonics have been completely canceled and that the contribution is negligible. The waveforms shown are practically sine waveform and the ripple completely disappears.

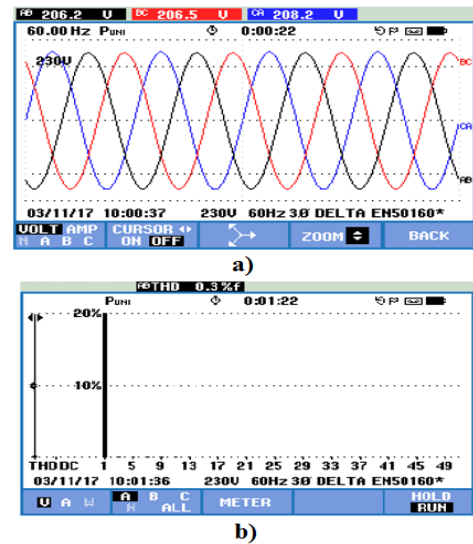


Fig.17.a) Line voltage waveform b) Line voltages spectrum with capacitive load.

The current is shown in Figure 18.a, it can be seen that the ripple appears again. However, as shown in Figure 18.b harmonics decreases respect to the lagging power factor test. This is because the presence of low-order harmonic components disappears. In Figure 18.b the spectrum expanded 20% to verify the presence of low-order harmonics. The THDi is only 1%, which confirms the optimization in the first 50 components.

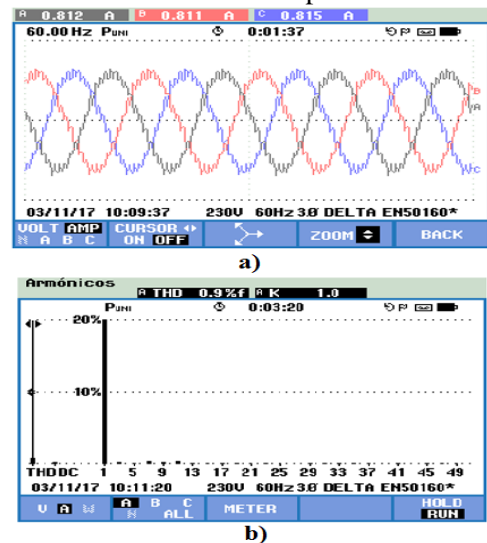


Fig. 18.a) Line current waveform b) Line current spectrum with capacitive load.

The phasor diagram of the voltages and currents measured in the test is shown in Figure 19. Although at first glance the system seems balanced, there are small differences in the voltages and currents, the unbalance of the line voltages has a value of 0.59%, and 0.2% of current, which is the lower unbalance registered. Voltage regulation has a value of 5.1%, which fully complies with the IEEE-1159 standard.



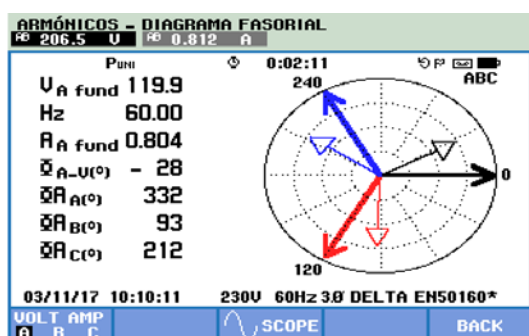


Fig.19. Phasor diagram for capacitive load.

### Test summary

A summary of all the tests is shown in Table II, factor imbalance and percent control are calculated as presented in [31]. This table shows that the THD of the phase voltages is quite high in all tests, but the THD of line that is optimized in that work oscillates at very low values of 0.3-0.6%.

TABLE II: Tests results summary

Variable	Parameter	Test			
		Noload	Resist.	Induc.	Capac.
Phase Voltage	Mean Vrms (V)	126.23	120.33	123.73	120.67
	% Regulation	0	4.67	1.97	4.4
	% Unbalance factor	1.28	1.27	1.15	0.63
	%THD <sub>v</sub>	10.9	11.6	11.2	11.5
Line Voltage	Mean Vrms (V)	218.1	206.86	212.86	206.96
	% Regulation	0	5.15	2.3	5.1
	% Unbalance factor	0.59	0.64	0.34	0.59
	%THD <sub>v</sub>	0.4	0.3	0.6	0.3
Line Current	Mean Irms (A)	0	0.716	1.08	0.81
	% Unbalance factor	0	0.41	2.68	0.2
	%THD <sub>i</sub>	0	0.5	2.3	0.9
	Output Power (W)	0	255.1	86.7	256
Power	Power Factor	0	1	0.22 L	0.88 C
	Reactive Power(VA)	0	255.1	397	291

Likewise, it is observed that the imbalances in the phase voltages and line meets EN50160 which establishes a maximum of 2%, as percentages of regulation which is maintained within the range established by the IEEE 1159 which states that the normal band operation voltage must be within 10% fluctuation.

## 9. Conclusions

The phase voltage THD in this work is quite high because the proposed optimization is directly in line voltages. The value of THD<sub>v</sub> phase ranged from 10.9% in the vacuum test and 11.6% in the test resistive load. This shows that the load disturbs the behavior of the converter; however variations are not very representative. As for the measured harmonic spectra phase voltages each of the tests demonstrated that the components present were triples because as deduced in mathematical modeling these harmonics would be eliminated in

the line voltages by the potential difference between the two phases.

THD of line voltages evidences good optimization performed by the algorithm, since all THD tests were below the limit set by the IEEE 519 which is 5%. The highest THD is at 0.6%, which is a very low value.

The results regarding the THD<sub>v</sub> voltage line reflects the good design of the converter, as this reproduces the waveforms calculated in an accurate manner, although the converter uses transformers; the same design minimizes perturbations they could generate, is for this reason that the THD is very low despite the presence thereof.

The optimization algorithm developed will be able to override all defined harmonic content between 2 and 50 if a sufficient number of shooting angles is given, however, modulations that are not possible to implement can occur.

The optimized theoretician THD of this project is defined as 0.00032% that this is the harmonic content of the modulation optimized to the 50<sup>th</sup> harmonic, being the upper bound of evaluation established by the IEEE 519.

From the experimental point of view the optimized THD for line voltage waveform is defined as 0.6% because this is the largest THD present in the tests.

The converter meets the quality standards of energy; this is why this converter is a good proposal to improve the quality of three-phase PV energy systems.

### References

- [1]. Mohammad Barghi Latran, Ahmet Teke, Investigation of multilevel multifunctional grid connected inverter topologies and control strategies used in photovoltaic systems, Renewable and Sustainable Energy Reviews, Volume 42, February 2015, Pages 361-376, ISSN: 1364-0321.
- [2]. P. Veena, V. Indragandhi, R. Jeyabharath, V. Subramaniaswamy, Review of grid integration schemes for renewable power generation system, Renewable and Sustainable Energy Reviews, Volume 34, June 2014, Pages 628-641, ISSN: 1364-0321.
- [3]. Abdelaziz Fri, Rachid El Bachtiri, Abdelaziz El Ghzizal, A Comparative Study of Three Topologies of Three-phase (5L) Inverter for a PV System, Energy Procedia, Volume 42, 2013, Pages 436-445, ISSN 1876-6102.
- [4]. Mohammad, S. Z.; Omar, A. N. and Ibrahim, I. R. "A Review of Single-Phase Single Stage Inverter Topologies for Photovoltaic System". 4th Control and System Graduate Research

- Colloquium, Shah Alam, Malaysia, Vol. 19, N. 20, Aug. 2013, pp. 69-75.
- [5]. Mehmet, Y.; Seydi, V.; Seci, V. and Hasan, C. "Comparison of Output Current Harmonics of Voltage Source Inverter used Different PWM Control Techniques". WSEAS Transactions on Power Systems Vol. 3, 2008. pp 696-703.
- [6]. Diaz Rodríguez, J. L., Pabon Fernández, L.D: y Pardo García, A. THD Improvement of a PWM Cascade Multilevel Power Inverters Using Genetic Algorithms as Optimization Method, Wseas Transactions On Power Systems ISSN: 2224-350X, 2015 voumenl:10 fasc: 1 Grecia pages: 46–54.
- [7]. T. Sudhakar Babu, K. Priya, D. Maheswaran, K. Sathish Kumar, N. Rajasekar, Selective voltage harmonic elimination in PWM inverter using bacterial foraging algorithm, Swarm and Evolutionary Computation, Volume 20, February 2015, Pages 74-81, ISSN 2210-6502.
- [8]. Abdul Moeed Amjad, Zainal Salam, A review of soft computing methods for harmonics elimination PWM for inverters in renewable energy conversion systems, Renewable and Sustainable Energy Reviews, Volume 33, May 2014, Pages 141-153, ISSN 1364-0321, <http://dx.doi.org/10.1016/j.rser.2014.01.080>.
- [9]. Anup Kumar Panda, Yellasiri Suresh, Research on cascade multilevel inverter with single DC source by using three-phase transformers, International Journal of Electrical Power & Energy Systems, Volume 40, Issue 1, September 2012, Pages 9-20, ISSN 0142-0615.
- [10]. Malinowski, M.; Gopakumar, K.; Rodriguez, J. and Pérez, M. "A Survey on Cascaded Multilevel Inverters", IEEE Trans. on Ind. Elect., Vol. 57, N. 7, July 2010, pp. 2197-2206.
- [11]. Ilhami Colak, Ersan Kabalci, Ramazan Bayindir, Review of multilevel voltage source inverter topologies and control schemes, Energy Conversion and Management, Volume 52, Issue 2, February 2011, Pages 1114-1128.
- [12]. Nayan Kumar, Tapas Kumar Saha, Jayati Dey, Modeling, control and analysis of cascaded inverter based grid-connected photovoltaic system, International Journal of Electrical Power & Energy Systems, Volume 78, June 2016, Pages 165-173, ISSN 0142-0615.
- [13]. Venkatachalam Kumar Chinnaiyan, Jovitha Jerome, J. Karpagam, An experimental investigation on a multilevel inverter for solar energy applications, International Journal of Electrical Power & Energy Systems, Volume 47, May 2013, Pages 157-167, ISSN 0142-0615.
- [14]. Bailu Xiao; Lijun Hang; Jun Mei; Riley, C.; Tolbert, L.M.; Ozpineci, B., "Modular Cascaded H-Bridge Multilevel PV Inverter With Distributed MPPT for Grid-Connected Applications," in Industry Applications, IEEE Transactions on , vol.51, no.2, pp.1722-1731, March-April 2015 doi: 10.1109/TIA.2014.2354396.
- [15]. Ajami, A.; Farakhor, A.; Ardi, H., "Minimisations of total harmonic distortion in cascaded transformers multilevel inverter by modifying turn ratios of the transformers and input voltage regulation," in Power Electronics, IET , vol.7, no.11, pp.2687-2694, 11 2014 doi: 10.1049/iet-pel.2013.0533.
- [16]. Baker R. H. y Lawrence H. B. Electric Power Converter, US. Patent Number 3,867,643, 1975.
- [17]. Nabae, A., Takahashi, I. and H. Akagi. "A new neutral point clamped PWM inverter", IEEE Trans. Ins. Appl., vol. IA-17, N. 5, pp.518-523, Sep-Oct, 1981.
- [18]. Odeh, C.I., "Improved three-phase, five-level pulse-width modulation switched voltage source inverter," in Power Electronics, IET , vol.8, no.4, pp.524-535, 4 2015 doi: 10.1049/iet-pel.2014.0133.
- [19]. Jin-Sung Choi; Feel-Soon Kang, "Seven-Level PWM Inverter Employing Series-Connected Capacitors Paralleled to a Single DC Voltage Source," in Industrial Electronics, IEEE Transactions on , vol.62, no.6, pp.3448-3459, June 2015 doi: 10.1109/TIE.2014.2370948.
- [20]. Fengjiang Wu; Xiaoguang Li; Fan Feng; Hoay Beng Gooi, "Modified Cascaded Multilevel Grid-Connected Inverter to Enhance European Efficiency and Several Extended Topologies," in Industrial Informatics, IEEE Transactions on , vol.11, no.6, pp.1358-1365, Dec. 2015, doi: 10.1109/TII.2015.2486623
- [21]. L. David Pabón Fernández, E. A. Caicedo y J. L. Díaz Rodríguez, "Comparative analysis of 9 levels cascade multilevel converters with selective harmonic elimination", Power Electronics and Power Quality Applications (PEPQA), IEEE Workshop on, Bogota, 2015, pp. 1-6, doi: 10.1109/PEPQA.2015.7168244.
- [22]. Banaei, M. R.; Khounjahan H. and Salary, E. "Single-source cascaded transformers multilevel inverter with reduced number of switches". IET Power Electron, Vol. 5, N. 9, 2012, pp. 1748- 1753.
- [23]. Diaz-Rodríguez, J. L.; Pabón-Fernández, L. D.; Caicedo-Peñaranda, E. A. Novel methodology for the calculation of transformers in power

multilevel converters. *Ingeniería y competitividad*, 2015, vol.17, n. 1.

- [24]. T. Sudhakar Babu, K. Priya, D. Maheswaran, K. Sathish Kumar, N. Rajasekar, Selective voltage harmonic elimination in PWM inverter using bacterial foraging algorithm, *Swarm and Evolutionary Computation*, Volume 20, February 2015, Pages 74-81, ISSN 2210-6502.
- [25]. M. Gnana Sundari, M. Rajaram, Sujatha Balaraman, Application of improved firefly algorithm for programmed PWM in multilevel inverter with adjustable DC sources, *Applied Soft Computing*, Volume 41, April 2016, Pages 169-179, ISSN 1568-4946.
- [26]. Debnath, S. Narayan, R. and Ghosh, T. "Comparison of Different Soft Techniques applicable to Multilevel Inverter for Harmonic Elimination". *International Journal of Computer Application*, Vol. 6, N. 2, Dec., 2012.
- [27]. M. Gnana Sundari, M. Rajaram, Sujatha Balaraman, Application of improved firefly algorithm for programmed PWM in multilevel inverter with adjustable DC sources, *Applied Soft Computing*, V. 41, April 2016, Pages 169-179, ISSN 1568-4946.
- [28]. Vivek Kumar Gupta, R. Mahanty, Optimized switching scheme of cascaded H-bridge multilevel inverter using PSO, *International Journal of Electrical Power & Energy Systems*, Volume 64, January 2015, Pages 699-707.
- [29]. IEEE Std. 519-1992-IEEE Recommended Practices and Requirements for Harmonic Control in Electrical Power Systems. IEEE, 1992.
- [30]. Diaz-Rodriguez, J. L.; Pabon-Fernandez, L. D. and Contreras-Pena, J. L. Plataforma de bajo costo para la evaluación de fenómenos electromagnéticos monofásicos de calidad de la energía según el estándar IEEE 1159. *Dyna rev.fac.nac.minas* [online]. 2015, vol.82, n.194 [cited 2016-03-27], pp. 119-129.
- [31]. Sánchez, M. A. *Calidad de la energía eléctrica*. Instituto Tecnológico de Puebla, México, 2009.